Battery Energy Storage System to Stabilize Transient Voltage and Frequency and Enhance Power Export Capability

Battery Energy Storage System to Stabilize Transient Voltage and Frequency and Enhance Power Export Capability

Ujjwal Datta, Akhtar Kalam, and Juan Shi

***Abstract*—This paper investigates the enactment of Battery Energy Storage System (BESS) and Static Compensator (STATCOM) in enhancing large-scale power system transient voltage and frequency stability, and improving power export capacity within two interconnected power systems. A PI-lead and lead-lag controlled BESS is proposed for multimachine power system to provide simultaneous voltage and frequency regulation within the defined battery state-of-charge (SOC) ranges and an equivalent Finnish transmission grid is used to evaluate the system performance. According to Australian National Electricity Market (NEM) grid requirements, the performances of the proposed control schemes are compared with conventional PI controlled BESS and STATCOM under multiple temporary and permanent fault conditions. In addition, two adjacent disturbance events are also applied to evaluate system performance with BESS and STATCOM. Through simulation results, it is shown that when there is a 44% increase in power export and the STATCOM fails, incorporating BESS improves the performance and justifies the novelty of this study. Moreover, the proposed lead-lag controlled BESS manifests better transient performance than BESS with PI-lead and traditional PI controller, in the event of divergent temporary and permanent faults.**

***Index Terms*—Battery energy storage system, frequency stability, PI lead controller, Lead-lag controller, power export, STATCOM, voltage stability.**

I. Introduction

THE present power transmission system is experiencing numerous control and stability challenges with growing energy demand and penetration of renewable energy resources (RES). Structural reform of vertically integrated traditional power system is very complex and challenging. The ever-increasing size and complexity of electric grid infrastructure has drawn much attention in power system operation, stability and performance as it is often susceptible to diverse small or large dynamic and transient disturbances that inevitably occur in power system. Deregulated electricity market and electricity pricing schemes cause unplanned exchange of power within the network. This may result in overloading certain lines of transmission network and may lead to system instability in the event of network faults. In addition, compelled by sustainable energy initiatives, large-scale PV and wind farms are often located far away from load center. Therefore, transmission system stability and reliability needs to be ensured to satisfy power system reliability requirement of (N-1) criterion in order to maximize the utilization of accessible transmission resources.

In the electric grid, every disturbance events, regardless of temporary or permanent in nature, generates low or high frequency oscillations. Flexible AC Transmission System (FACTS) devices have been contributing significantly in enhancing power system transient stability (low/high order oscillation) by regulating power flows and enhancing power transfer capacity of transmission system [1]–[3]. Among the multiple FACTS devices, the particular interest of this study is on static synchronous compensators (STATCOM) as this device improves power transfer capability [4], [5], enhances transient stability by regulating voltage [6], ameliorates inter-area oscillation [7] and provides faster and smoother voltage recovery through reactive power compensation [8]. In addition, STATCOM outperforms other FACTS devices in damping power system oscillations [9] and enhancing power transmission capacity in many occasions [10].

In comparison to STATCOM, BESS principally plays divergent role in power system i.e. frequency control [11], active power output smoothing in RES farm [12], transient stability improvement [13], improving the damping of electromechanical power oscillation [14], [15], and providing voltage and power quality support. Kawabe et al. [13] have indicated that BESS improves transient stability whereas Setiadi et al. [14] concluded that BESS provides better electromechanical oscillation damping performance than power system stabilizer (PSS). Maleki et al. [15] have shown that BESS provides better power oscillation damping than STATCOM in a single machine infinite bus (SMIB) power system. In many occasions, STATCOM with super-capacitor [16] or battery [17] is proven to be more efficient than a standalone STATCOM mainly in RES integrated system. In particular, BESS has been mainly investigated in improving transient stability and power oscillation damping. In this frame of reference, the application of BESS in providing power system transient stability and enhancing power transfer capability within interconnected power systems is relatively a new area of interest and it is to be explored thoroughly. A study in [18] demonstrated that BESS can reduce network congestion and defer network expansion planning. The authors in previous study [19] demonstrated that BESS can effectively stabilize transient frequency and enhance power export in the

This work was supported by the Victoria University International Postgraduate Research Scholarship (IPRS) scheme. The authors are with the College of Engineering and Science, Victoria University, PO Box 14428, Melbourne, Australia, 8001. Ujjwal Datta (e-mail: Ujjwal.datta@live.vu.edu.au). Akhtar Kalam (e-mail: Akhtar.Kalam@vu.edu.au). Juan Shi (e-mail: Juan.Shi@vu.edu.au).

event of permanent disturbance. Kanchanaharuthai et al. [20] have shown that STATCOM with battery storage outperforms PSS in reducing power system oscillations. In another study, Beza et al. [21] demonstrated that STATCOM with energy storage provides effective power oscillation damping. However, in earlier studies [13]-[17], power transfer capacity was not investigated. Moreover, the studies in [20] and [21] did not perform comparative stability analysis between STATCOM and BESS in terms of their impact on power transfer within interconnected power systems under permanent disturbance events in view of issues of simultaneous voltage and frequency stability.

Several research works have been carried out in regulating voltage and frequency to enhance the damping capability of the power system. Authors in [22]–[24] demonstrated that STATCOM with BESS can improve the damping of voltage and frequency or power. However, the studies either did not consider battery SOC or considered as a constant value which is not considered in a real power system. Moreover, only the conventional PI is applied to regulate BESS [23], [24] and also the proposed BESS control is prone to rapid charging/discharging as no deadband is employed in the design [22]–[24]. Active or reactive power priority controlled BESS in an isolated power system is investigated in [25] for regulating frequency or voltage, one at a time. STATCOM with BESS in a large-scale power system is proposed in [26] where BESS is employed either as an active or reactive power stabilizer to reduce inter-area oscillations. However, coordinated voltage and frequency regulation and battery SOC are not considered in the study. The prior studies come with the shortcomings of lack of simultaneous voltage and frequency regulation or battery SOC consideration or equivalent performance analysis between STATCOM and BESS in increasing active power between two areas of large-scale systems.

In this paper, comparative performance of STATCOM and BESS in enhancing power transfer capability across interconnected electric grid is explored. This paper investigates the performance of STATCOM and BESS in enhancing transient stability, making contribution in voltage and frequency regulation to support the increased amount of power export between two large-scale interconnected power systems, with the conventional synchronous generators and RES. The impact of disturbance events such as temporary and permanent short circuit faults, permanent line outage are considered for transient stability analysis following voltage and frequency operating standards published by the Australian Energy Market Operator (AEMO) according to NEM policy [27], [28]. The main contributions of this paper are summarized as follows:

- The evaluation and comparative performance analysis between STATCOM and BESS is to enhance transient stability and support the increased amount of power transfer between interconnected power systems, under various temporary and permanent contingencies. BESS is designed to provide simultaneous voltage and frequency regulation and operate within the defined SOC operating ranges and this research has not been reported in current literatures.
- PI-lead and lead-lag controlled BESS are proposed in this study and to the authors' best knowledge these types of controllers have not been applied to BESS to regulate both the voltage and frequency simultaneously by controlling BESS active and reactive power. The design effectiveness is compared to conventional PI controlled BESS in stabilizing voltage and frequency of a large-scale real power system and enhancing power transfer capability of the power system.
- The analysis of the impact of multiple adjacent disturbance events on the transient stability and the efficacy of state-of-the-art STATCOM technology and BESS with the proposed control strategies to avoid blackout that has been neglected in earlier studies of power system stability analysis.

To evaluate the performance of BESS with the proposed control approaches and STATCOM in enhancing transient stability, multiple case studies have been carried out using an equivalent 400kV Finnish transmission grid and comparative performances are evaluated and presented. The rest of the paper is outlined as follows: detail modeling of BESS is described in section II, the test network and stability criterion are explained in section III, results and discussion are described in section IV and the conclusion is drawn in section V.

II. Detailed Modeling of BESS with the Proposed Controllers

The BESS model includes battery bank, a three-phase bi-directional DC/AC converter and a three-phase step up transformer connecting BESS into the system. In this section, the modeling and detail control techniques of BESS are discussed. Fig. 1 illustrates the BESS structure used in this study. Active power support to control frequency is limited by battery capacity and reactive power support is limited by the PWM converter capacity. BESS can provide voltage and frequency support as its features allow the ability to control the active and reactive power independently by two separate current parameters in d and q axis within converter capacity. The main BESS controller design is divided into 6 different segments and those are explained in detail as follows:

A. Frequency controller
B. Voltage controller
C. Active/reactive (PQ) power controller
D. Charge controller
E. d and q axis current controller
F. Battery model

A. Frequency Controller

Frequency Controller as shown in Fig. 2 generates active power control reference based on the frequency error between the grid and the nominal frequency beyond deadband limit according to the droop setting.

Active power supply (discharging) and consumption (charging) are controlled by positive and negative error (f_{error}) value, given that sufficient battery capacity is available.

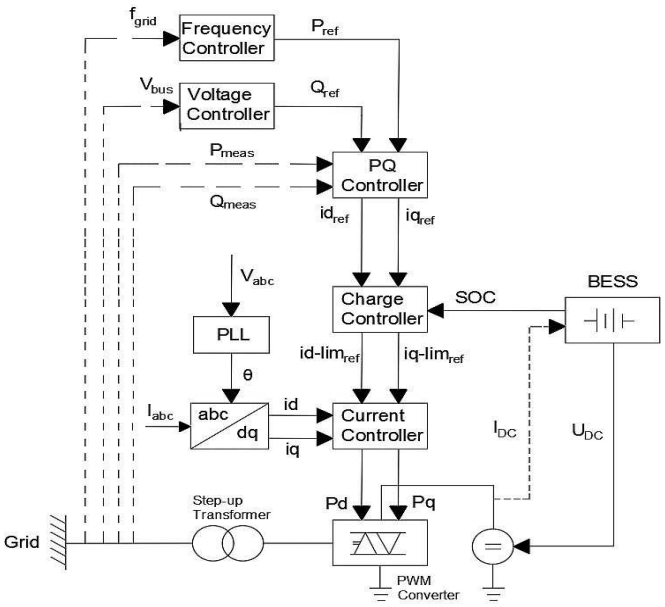

Fig. 1. Schematic of a BESS and its control

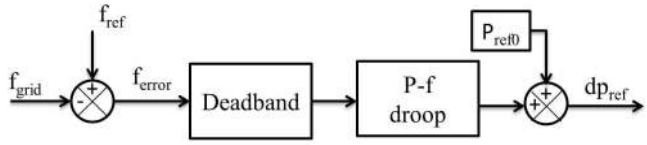

Fig. 2. Frequency controller model

B. Voltage Controller

The voltage controller as shown in Fig. 3 generates reactive power control signal reference depending on error between the actual bus and the nominal reference voltage according to droop value and the direction of reactive current is regulated with respect to a positive and a negative value of v_{error}.

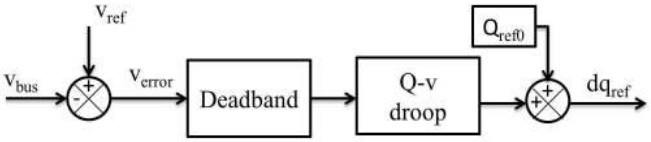

Fig. 3. Voltage controller model

The local voltage and frequency measurement at BESS connected point (central-north bus) are selected as input signals to generate and control BESS active and reactive power.

C. Active/Reactive (PQ) Controller

Once the voltage and frequency controller initiates active and reactive power signal, the PQ controller will produce the control signal. Frequency and P controller serve the same purpose of generating active power control signal whereas voltage and Q controller initiates reactive power signal. However, the input signals are different for each controller. Two new control strategies are proposed in PQ controller along with the conventional PI controller. The detail working strategies of the proposed controllers can be found in the articles [29]–[33]. The output power at BESS AC terminal is measured and compared with the active power activation signal. The "Δi_d" signal from the charge controller is added and then used as an input to PI/PI-lead/lead-lag controller to generate active power reference signal. For reactive power control, "Δi_q" signal is added to PI/PI-lead/lead-lag controller input to generate reactive power reference signal.

1) Anti-windup PI controller: An anti-windup limiter is utilized with the conventional PI controller to avoid integrator windup as shown in Fig. 4.

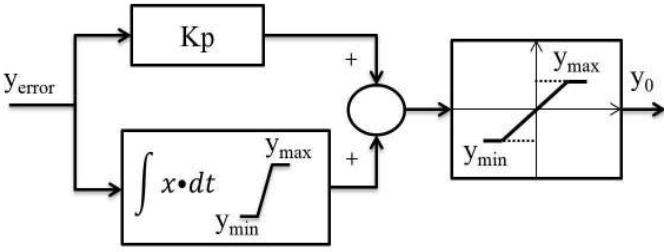

Fig. 4. PI controller with anti-windup on power limits

The equation of PI controller with anti-windup [29], [30] can be written as :

$$y_o = \left[K_p * y_{error} + \frac{K_i}{Ti} \int_{y_{min}}^{y_{max}} y_{error}\ dt \right]_{y_{min}}^{y_{max}} \tag{1}$$

where, y_o=i_{d-ref}=i_{q-ref} at PQ controller output, y_{max}=i_{d-max}=i_{q-max} and y_{min}=i_{d-min}=i_{q-min} for d and q axis.

The PQ controller with conventional PI is shown in Fig. 5. Each PI controller in d and q axis are mainly independently controlled in PQ controller. However, they are coordinated and regulated by the current limiter in the charge controller where the reference current on d and q axis are calculated to ensure converter operation within the converter capacity. The PI controller parameters (which are tuned by Ziegler-–Nichols method) are given in Appendix A. The time constant in the first order filter significantly affects the dynamic behavior and therefore larger time constant value results slower transient response.

2) PI-lead controller: PI-lead controller is a composite of PI and Lead controller connected in series as shown in Fig. 6. The lead controller yields better transient system response i.e. reduces overshoot and settling time by contributing improvements in phase margin. The lead controller transfer function for d and q axis are given as:

$$K_1(s) = \frac{T_{b1}}{T_{a1}} \frac{(s + 1/T_{b1})}{(s + 1/T_{a1})} \tag{2}$$

$$K_2(s) = \frac{T_{b2}}{T_{a2}} \frac{(s + 1/T_{b2})}{(s + 1/T_{a2})} \tag{3}$$

DC gain= 1. T_{b1}>T_{a1} and T_{b2}>T_{a2}.

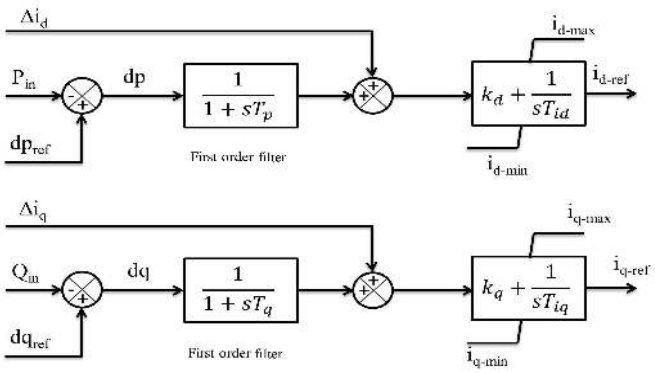

Fig. 5. PQ controller with conventional PI control

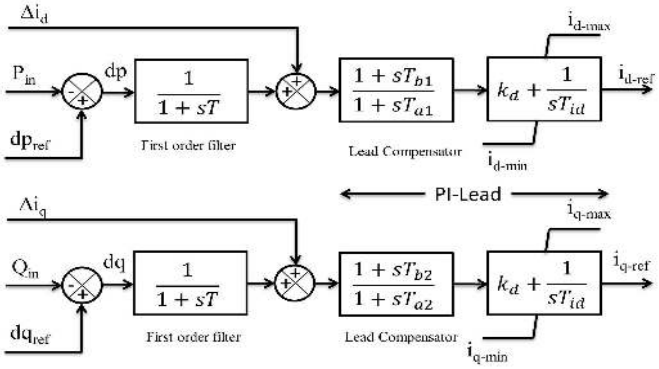

Fig. 6. PQ controller with PI-lead control

In a lead compensator, the zero is placed closer to the origin than the pole and provides faster response by shifting the closed loop poles to the left of left hand s-plane. The detailed discussion on lead controller and PI-lead can be found in [31], [32]. To contribute in improved system response, a lead controller is added with conventional PI to regulate active/reactive power of BESS. The pole and zero locations are tuned through iterative process whereas PI parameters remain the same as in the conventional PI controller. The transfer function of the designed PI-lead controller for d and q axis are the same and can be written as follows:

$$K(s) = \frac{1+s}{1+0.5s} = \frac{2(s+1)}{(s+2)} \tag{4}$$

3) Lead-lag controller: With non-stationary behavior of the power system, in many occasion PI controller fails to accomplish its purpose of stability improvement. Considering such limitation of PI controller, a lead-lag controller is proposed in this study as shown in Fig. 7. A Lead-lag controller is a combination of lead and lag controller to attain solitary benefit of reduced steady-state error i.e improved and reliable system stability and faster transient response by eliminating each controller's drawbacks. The detail working principles of a lead-lag controller can be found in [32], [33]. The limiter controls the output power reference within predefined boundary. The associated lead-lag parameters are listed in Appendix A.

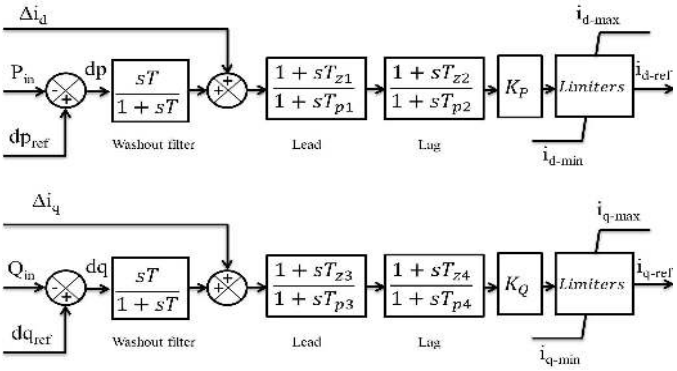

Fig. 7. PQ controller with lead-lag control method

The poles/zeros are determined by trial and error. The transfer function of the proposed lead-lag controller for d-axis is:

$$K_1(s) = \frac{T_{z1}}{T_{p1}} \frac{(s+1/T_{z1})}{(s+1/T_{p1})} \frac{T_{z2}}{T_{p2}} \frac{(s+1/T_{z2})}{(s+1/T_{p2})} \tag{5}$$

where DC gain= 1. T_{z1}>T_{p1} (lead) and T_{p2}>T_{z2} (lag). The transfer function of the proposed lead-lag controller for q-axis is:

$$K_2(s) = \frac{T_{z13}}{T_{p3}} \frac{(s+1/T_{z3})}{(s+1/T_{p3})} \frac{T_{z4}}{T_{p4}} \frac{(s+1/T_{z4})}{(s+1/T_{p4})} \tag{6}$$

The lead-lag controller with the designed poles/zeros locations for d and q axis are as follows:

$$K_1(s) = K_2(s) = \frac{8(s+1)(s+0.25)}{(s+2)(s+0.067)} \tag{7}$$

with T_{z3}>T_{p3} (lead) and T_{p4}>T_{z4} (lag).

D. Charge Controller

The first block of charge controller is SOC control which defines BESS active power participation i.e. charging or discharging conditions according to frequency oscillation beyond nominal value (positive or negative) as shown in Fig. 5. BESS can consume active power if battery SOC is less than the maximum SOC limit and can supply active power if SOC is greater or equal to the minimum SOC level to comply with safe depth-of-discharge of battery. In this study, the values for the maximum and the minimum SOC is selected as 100% and 20%.

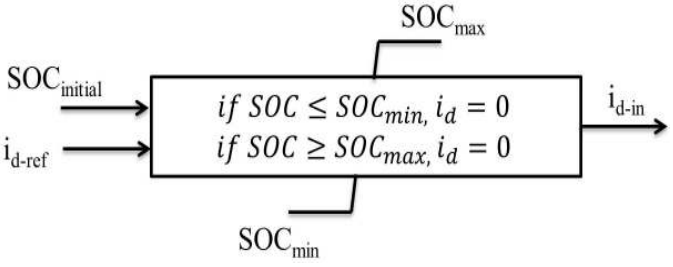

Fig. 8. SOC control strategy

The active power contribution of BESS is delimited by SOC level and therefore, the current reference on d-axis are executed according to the conditions specified as follows:

$$i_{d-in} = \begin{cases} i_{d-ref} & SOC_{min} \leq \text{SOC} \leq SOC_{max} \\ 0 & \text{otherwise} \end{cases}$$

The second block as shown in Fig. 9 illustrates the maximum value of absolute current which is a function of d and q axis current reference. The charge controller block diagram is shown in Fig. 6. The difference between "i_{d-ref}" and "$i_{d-ref-out}$ of charge controller "Δi_d" is added with active power reference input in PQ controller. The difference between "i_{q-ref}" and "$i_{q-ref-out}$" of charge controller "Δi_q" is added with reactive power reference input in PQ controller.

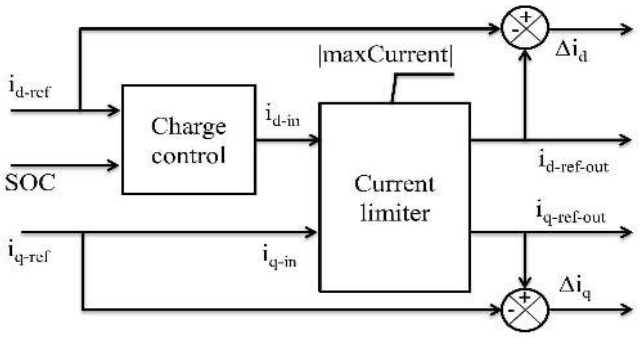

Fig. 9. Charge controller model

The BESS apparent power is limited by the converter capacity. Therefore, the summation of total current on d and q axis must be equal to the nominal value of the converter to avoid converter overloading. Hence, the total current should be equal to the maximum absolute value (maxValue) of 1 per unit. The coordination between d and q axis current are calculated as follows:

$$i_{d-ref-out} = \int_{-|maxValue|}^{|maxValue|} i_{d-in}\, dt \tag{8}$$

$$i_{q-ref-out} = \int_{-y_{value}}^{y_{value}} i_{q-in}\, dt \tag{9}$$

where, $y_{value} = \sqrt{\left| \int_{0}^{|maxValue|^2} |maxValue|^2 - i_{d-in}^2 \right|}$

E. d and q axis Current Controller

The main characteristics of dq current controller is its capability to adjust BESS active and reactive power by regulating d and q axis current component based on PI controller output as shown in Fig. 10. The controller input currents are the converter's AC current in dq reference frame. The voltage angle is calculated using Phase-locked-loop (PLL) and the output is connected to a reference system to define transformation between dq reference frame and global reference frames. The output signal is pulse width modulation index on d-axis (m_d) and q-axis (m_q).

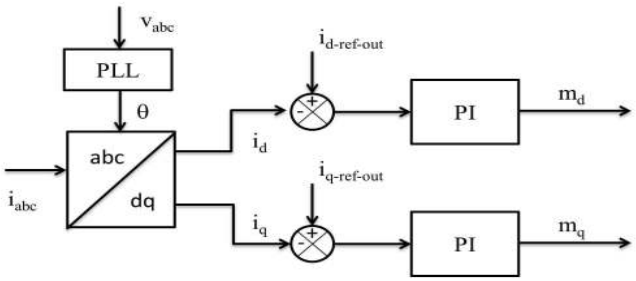

Fig. 10. d and q axis current controller model

F. Battery Model

The battery model used in this paper is an electrical equivalent battery model described in [34] where the battery is modeled as a DC voltage source and an internal resistance where SOC of the battery is a function of battery current.

III. System Description and Transient Stability Criterion

A. System Configuration

An equivalent representation of Finnish transmission network is considered in this study to investigate the contribution of BESS and STATCOM devices. The schematic diagram of the studied transmission system is shown in Fig. 11 which comprises of 15 equivalent synchronous generators, 7 series capacitors and 11 equivalent loads. Capacitors parameters, active and reactive power of generators and loads are given in Appendix A. The other associated parameters of generators, generator step-up transformers (13.8/400kV), step-down transformers at load terminal (400/110kV) and transmission lines are available in [35].

The electrical parts of synchronous generator at north area (North-West (NW), North (N), North-East (NE), and Central-North (CN)) of the grid are represented by 5th order state-space models and the mechanical parts are represented by hydro type turbine and governor systems. The synchronous generators' electrical parts in Nordic (Nordic N1, Nordic N2, Nordic S and Nordic C) are represented by 6th order state-space models and the mechanical parts are represented by hydro type turbine and governor systems. The synchronous generators' electrical parts in central (Central-West (CW), Central (C), Central-South (CS) and Central-East (CE)) and south (South-West (SW), South (S) and South-East (SE)) are represented by 6th order state-space models and operating as constant torque. IEEE-AC5A type exciter is chosen for South-West generator and ST2A type exciter is used for the rest of generators.

The generators are coupled at 13.8kV bus and connected to 400kV system through a step-up transformer. The 4 generators in Nordic region are an equivalent representation of Swedish generation system. The generator at SW terminal (SW-gen) is considered as reference machine for the network whereas other generators are designed as PV at their local bus. There are no PSS installed at generators' terminal. Transmission lines between south area to CE, CS, CW, CS to C and Sirttoverkko

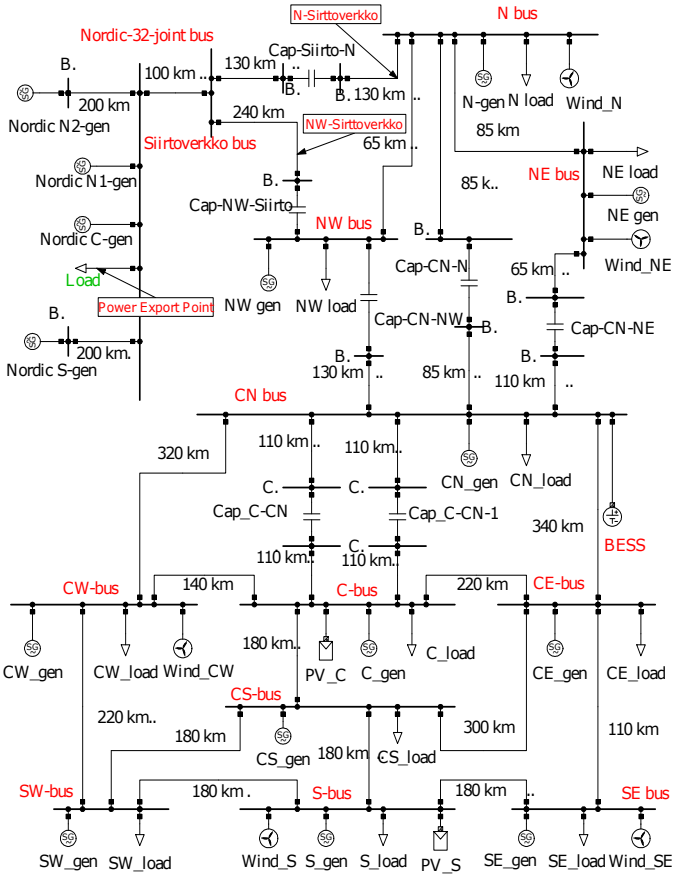

Fig. 11. Modified Finnish equivalent transmission network

to Nordic area comprised of two parallel lines whereas all other transmission lines are composed of single line. Three phase balanced load with active and reactive power is selected in this study. The loads are connected at 110kV level.

B. STATCOM and Wind Model

The basic STATCOM diagram consists of a DC source to supply constant voltage to voltage-source converter (VSC). This VSC converts DC/AC output whose AC terminal is connected to the transformer which acts as an interface between the VSC and the AC grid. The modelling details of STATCOM used in this paper can be found in [36]. The local measurements at STATCOM connected point (Central-north bus) are selected as input signal to control STATCOM. Doubly fed induction generator (DFIG) based wind turbine generator is used for wind farm modeling. The wind farm is designed to remain connected during fault period and is considered as operating at constant wind speed i.e. constant output.

C. Stability Criterion

The power system oscillatory response must be contained within the boundary, in the occurrence of single/multiple contingency events, to comply with the grid operating standards. Presently, successful frequency control according to the NEM requires that system frequency should be maintained between 0.99-1.01 pu of the nominal value within 1 minute for network event and should recover between 0.997-1.003 pu within 5 minutes as shown in Fig. 12. In the case of multiple contingency events, post-fault frequency should be between 0.99 and 1.01 pu within 2 minutes and 0.997-1.003 pu within 10 minutes [27]. The proposed operation limit of voltage by the AEMO is $\pm$ 10% of the nominal value with disturbance events for the duration of 20 minutes [28]. The power system should not exceed voltage and frequency operating standards in any circumstances. Following an contingency event, if the voltage and frequency reaches to the recovery band, the power system is stabilized and considered as sufficiently secure.

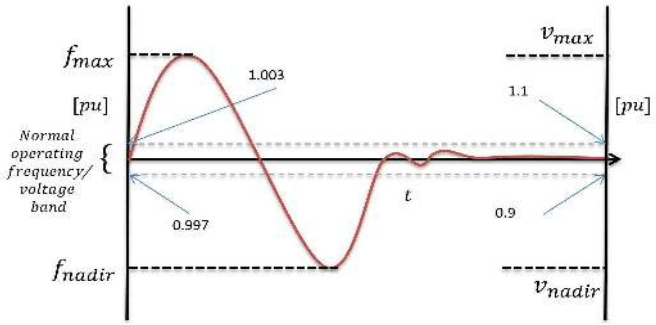

Fig. 12. NEM voltage and frequency operating standards

The amount of power transfer within areas are limited by transient voltage and frequency stability that apparently depends on overall system conditions and parameters at any given point in time. An extensive simulation study by AEMO demonstrated that loss of line outage significantly affects the power transfer limit to satisfy and keep the system within grid specified restrictions [37]. In addition, multiple outage events are more severe in limiting the maximum amount of power transfer compare to single outage event for meeting transient stability requirements [38]. Therefore, the contribution of single/multiple outage events are imperative to investigate as they can have severe consequences in power system stability such as blackout [39].

Traditionally, STATCOM is one of the state-of-the-art technologies that are being preferred in providing transient stability to provide better oscillation damping and enhancing power export in the grid. In this research, the effectiveness of BESS undergoing temporary and permanent single/multiple contingencies is the prime focus. Stability margin of the studied network with the integration of STATCOM and BESS will be evaluated according to NEM stability criteria as presented in Fig. 12.

IV. Results and Analysis

In this study, the performance of STATCOM and BESS with the proposed control strategies are evaluated on an equivalent real power system and comprehensive analysis of power export cases are evaluated using simulation studies following multiple transient events. The study encompasses the identification of maximum power export within large network from south area to north area in Nordic border. Afterwards, with increased volume of power export, stability support from STATCOM

and BESS is investigated to restore system stability following disturbances. Since the two networks are connected by two transmission lines, therefore they have significant impact on system stability.The performance of BESS with the proposed controllers (BESS with PI-lead and Lead-lag) are compared with the STATCOM and conventional PI controlled BESS.

Three studies (Cases I-III) are investigated to assess the control performance of STATCOM and BESS with the proposed control strategies to provide system stability. In addition, three other studies (Cases IV-VI) are investigated to establish BESS efficiency in transient stability enhancement.

- Case I: Fault of N-Sirttoverkko line and fault clearing by loss of line permanently (single support).
- Case II: Load growth, fault of N-Sirttoverkko line and fault clearing by loss of line (multiple supports).
- Case III: Fault of N-Sirttoverkko line, fault clearing by loss of line and load growth (multiple supports).

The Effectiveness of BESS in other transient conditions:

- Case IV: Temporary single-phase short circuit fault.
- Case V: Permanent single-phase short circuit fault.
- Case VI: Without series compensation between two systems.

To identify the stable operation limit of grid, different amount of active power export cases are investigated. The generators at South-West, South and South-East supplies 50MW, 200MW and 200MW of the total exported power to the power export point in Nordic region. In the fault simulation study a three-phase fault is applied at t=3s on N-Sirttoverkko line which is carrying about 220.7MW power and the fault is cleared at t=3.1s by removing faulted line permanently. From simulation results, it is identified that without any support from STATCOM/BESS devices, 450MW power export is the maximum power transfer limit following a line fault and permanent loss of the faulted line. Therefore, to investigate STATCOM/BESS contribution, higher amount of power is exported and STATCOM/BESS devices are placed.

A. Case I: 650MW export and Permanent loss of N-Sirttoverkko line

To substantiate STATCOM/BESS impact in enhancing power export within the network, 650MW active power export is considered. The active power contribution of SW generator is increased to 250MW, whereas generators at South and South-East supplies 200MW individually. When 650MW power is exported, three-phase line fault at t=3s on N-Sirttoverkko line is applied. The line is carrying about 321MW. The PCC voltage and generator frequency plots at different location shows that because of inadequate damping contributed by the generator excitation systems, system becomes unstable with 44.44% higher power export than stable condition when faulted line is permanently removed at t=3.1s to clear line fault as shown in Fig. 13. The system does not settle down within the grid required level and the time frame as mentioned in Fig. 12. This emerged instability requires to be settled to ensure the opportunity of higher power transfer across two interconnected systems and thus an additional damping support is required. The STATCOM and BESS is integrated at CN bus to provide supplementary damping into the system to mitigate the instability phenomena that emerges during higher order power exchange and unintended disturbance events. The location of STATCOM/BESS is selected based on overall satisfactory performance for all of the case studies through iterative process.

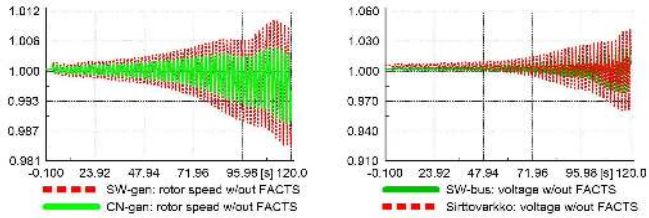

Fig. 13. The frequency of generators [p.u.] and voltages [p.u.] at bus and PCC without STATCOM/BESS support

STATCOM has proven its ability to increase power transfer capability in power system. A 80MVA STATCOM is integrated at CN bus to contribute in added damping and support system stability. The relative PCC voltage and generator frequency with incorporated STATCOM is shown in Fig. 14. It is observed that STATCOM fails to provide sufficient system damping and stabilize system responses. The post fault output responses of the system remain oscillatory and never settles down within the specified stability recovery band as mentioned in NEM regulations [27], [28]. Relatively, a large size of STATCOM is chosen to provide system damping. However, it is observed that even the large size of STATCOM remains ineffective to stabilize the post fault system responses.

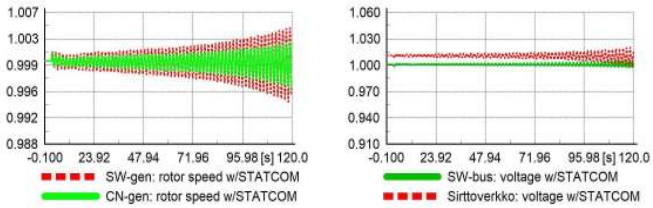

Fig. 14. The frequency of generators [p.u.] and voltages [p.u.] at bus and PCC with STATCOM

STATCOM delivers nil active power and 80MVAR reactive power. Therefore, it is evident that unavailability of active power results in the failure of STATCOM when stabilizing the system. Hence, a STATCOM is incapable to enhance network power export capability in a situation when voltage and frequency is affected by the disturbance. As a result, there is a requisite of active and reactive power provision to supply sufficient systems damping and stabilize system voltage and frequency.

BESS is integrated at CN bus to provide active and reactive power oscillation damping. Simulation results with integrated BESS as shown in Fig. 15 illustrates that BESS effectively contributes in system damping and stabilizes system voltage and frequency within the specified system recovery band as demonstrated in Fig. 12 while exporting 650MW across the interconnected network. The system responses reaches post

fault stability margin with the integrated BESS. Thus, the incorporated BESS improves power system stability with the proposed control strategies. To evaluate the transient stability responses, BESS with the proposed controllers are compared with conventional PI controlled BESS. As shown in Fig. 15, the proposed controllers not only stabilizes system responses Fig. 15 (a) but also BESS with lead-lag provides improved responses compare to BESS with conventional PI and PI-lead Fig. 15 (b).

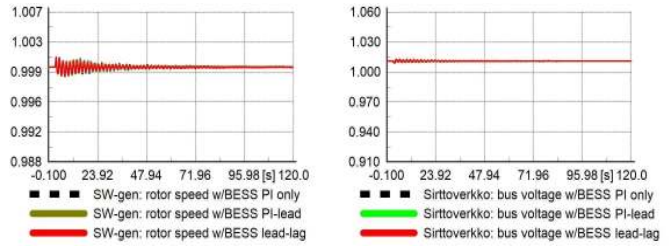

(a)

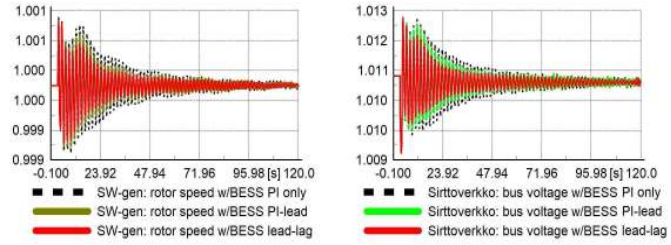

(b)

Fig. 15. The frequency of generators [p.u.] and voltage oscillations [p.u.] at bus and PCC with BESS (a) and responses with PI, PI-lead and lead-lag controlled BESS (b)

The active and reactive power by BESS is shown in Fig. 16. It can be seen that a very small amount of active power output is available with PI controlled BESS, this is due to limitation of PI controlled controller which is dependent on operating strategies and load and may not work satisfactorily for all conditions. On the contrary, the lead-lag controlled BESS output power is zero once the system stability is achieved, and this indicates robust control efficiency than conventional PI controlled BESS. It is observed that battery SOC does not change significantly as essentially high power is indispensable and BESS operation is required few seconds to few minutes. Mainly, turbine and governor system will strive to damp out oscillation in the case of energy surplus or shortfall beyond the battery capacity. A minimum size of BESS is essential to ensure sufficient BESS capacity (required SOC level) is obtainable for participating in transient stability enhancement. Therefore, a large size of battery capacity is considered to avoid surplus/shortfall during the studied transient periods. The size of BESS is selected considering all the case studies and the selected BESS converter is rated as 40MVA. The deadband for BESS active power triggering is $\pm$ 0.0002 p.u. of grid frequency value. The selected frequency droop value is 0.002 p.u. which defines that in a 50Hz frequency system, full BESS power is activated with $\pm$ 0.1Hz frequency deviation. On the contrary, the reactive power support capability of BESS is limited by the converter capacity. Deadband value for reactive power triggering is $\pm$ 0.004 p.u. value of nominal voltage at BESS connection point and droop value is 0.08 p.u. which defines full reactive power activation the minute voltage differs $\pm$ 8% of nominal bus voltage. Higher value of reactive power droop is selected to avoid excessive use of BESS converter for reactive power as grid voltage fluctuates often above/below 1 p.u. value. However, these droop values can be adjusted based on grid code requirements. The battery parameters are given in Appendix A.

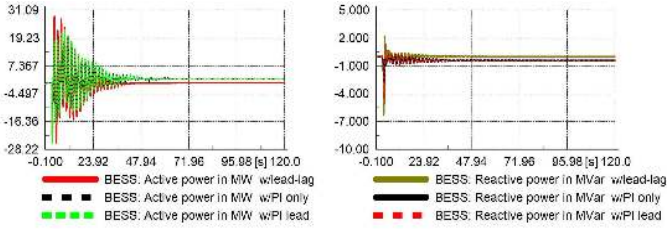

Fig. 16. BESS active and reactive power

In summary, comparative analysis between STATCOM and control strategies of BESS demonstrates that BESS not only stabilizes system voltage and frequency to continue power export but also maximizes the utilization of available transmission line power transfer capacity. Therefore, a STATCOM cannot compete with BESS in enhancing higher power export and hence, BESS has higher potential to be applied on grid level stability support than a STATCOM in such a case. At steady state operation, loading of N-Sirttoverkko line is 15.3% while NW-Sirttoverkko line is 17.4%. The minute N-Sirttoverkko line is lost after fault clearance, loading for the NW-Sirttoverkko increases to 32.4% which clearly evidents the above claim of BESS effectiveness in enhancing transient stability and power transfer capacity.

B. Case II: Loss of N-Sirttoverkko line and load growth at NW bus

Considering the impact of multiple disturbance events on transmission line [38], [39], STATCOM and BESS effectiveness are analyzed during two different faults in a row while exporting power within areas. The disturbance events are applied at about 20s apart from each other and the occurrence order of two events are reversed in two separate simulations. Simulation results are presented and discussed to demonstrate the feasibility of BESS in providing multiple stability services in a row. With the same amount of power being exported (650MW), a three-phase fault is applied on N-Sirttoverkko line at t=3s, fault is cleared at t=3.1s by removing faulted line and 10% active and reactive power increment in North-West load demand (about 30MW and 20MVAR) is activated at t=23.1s. Simulation results with multiple contingency events in Fig. 17 (a and b) show that without a BESS, system damping is not sufficient to stabilize the system responses that leads to escalating oscillations and fails to reconcile within the grid recovery voltage and frequency band according to NEM stability criteria mentioned in Fig. 12.

However, the results shown in Fig. 18 illustrates that a 40MW integrated BESS at CN bus provides adequate system

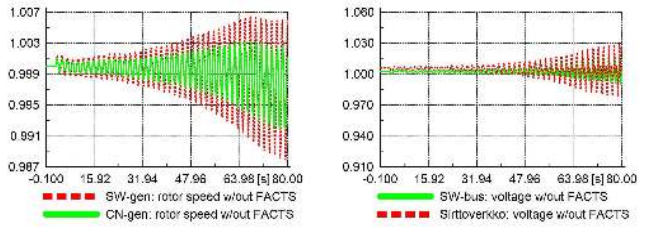

(a)

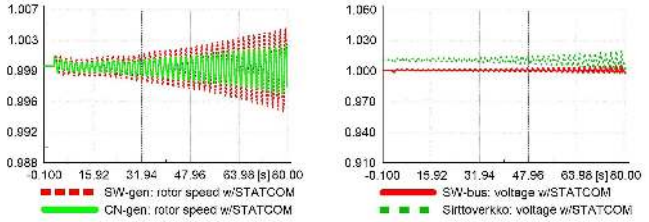

(b)

Fig. 17. The frequency of generators [p.u.] and voltage oscillations [p.u.] at bus and PCC without STATCOM support (a) and with STATCOM (b)

damping to stabilize post fault system responses in the case of multiple disturbances and ensures uninterrupted power export. The system responses demonstrate that according to NEM criteria, BESS with the proposed control approaches achieves power system stability. The droop values in this case study are the same as in Case I. The total active and reactive power of

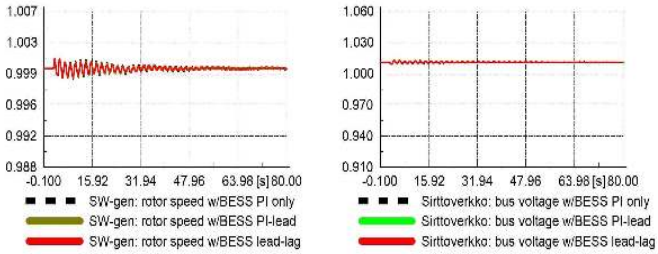

Fig. 18. The frequency of generators [p.u.] and voltage oscillations [p.u.] at bus and PCC with PI, PI-lead and lead-lag controlled BESS

BESS are shown in Fig. 19. In the case of PI controlled BESS, the output power of BESS does not settle to zero at post fault steady state whereas lead-lag controlled BESS output settles down to zero.

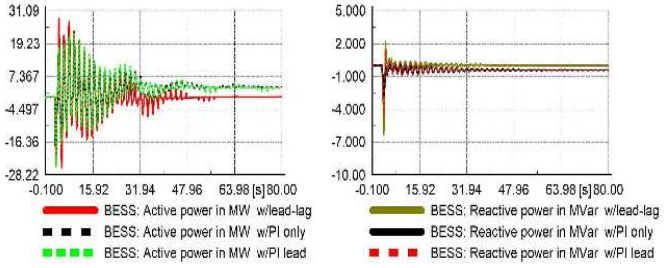

Fig. 19. BESS active and reactive power

C. Case III: Load growth at NW bus and loss of N-Sirttoverkko line

In this case study, the orders of disturbance events are reversed as in Case II. A 10% load increment is applied at t=3.1s and three-phase fault on N-Sirttoverkko line is applied at t=23s and the fault is cleared at t=23.1s by removing the faulted line permanently. The system responses with multiple fault events without BESS illustrates an accelerating oscillatory behavior and due to insufficient damping, voltage and frequency of the system never resolved within grid required band and continues toward instability as shown in Fig. 20 (a and b).

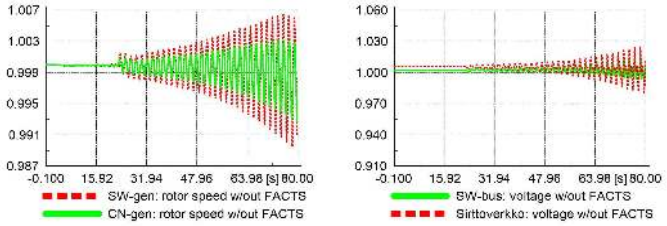

(a)

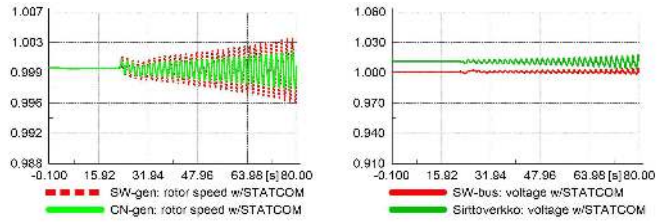

(b)

Fig. 20. The frequency of generators [p.u.] and voltage oscillations [p.u.] at bus and PCC without STATCOM support (a) and with STATCOM (b)

Simulation results in Fig. 21 illustrates that BESS installed at the same location as in previous case study turns out to be successful in stabilizing system voltage and frequency responses in the case of multiple disturbance events in a row. BESS delivers the required damping to the system and reduces the transient oscillation within the grid required recovery band that clarifies the stability achievement of BESS with the proposed control approaches. Same droop value for voltage and frequency is chosen as in Case I. BESS active and reactive power are shown in Fig. 22. A very similar behavior can be seen for active power output of PI controlled and lead-lag controlled BESS as in previous study.

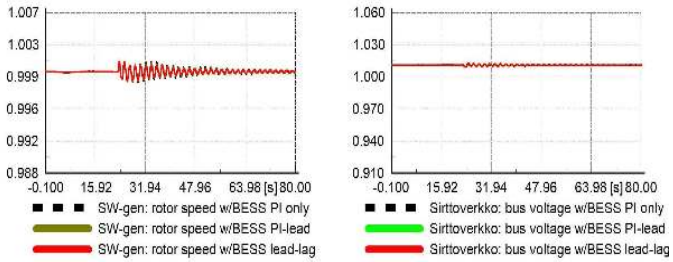

Fig. 21. The frequency of generators [p.u.] and voltage oscillations [p.u.] at bus and PCC with PI, PI-lead and lead-lag controlled BESS

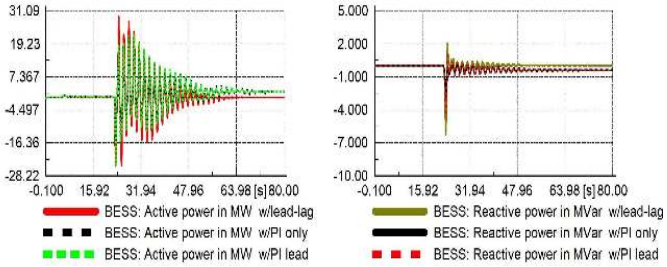

Fig. 22. BESS active and reactive power

A report from Australian Energy Market Operator (AEMO) on South-Australia blackout has identified that multiple transmission line faults are recorded within 87 seconds in the transmission network. These faults caused a reduction in generation and an increase in power transfer. The line outage from the persisted faults in such condition has resulted in voltage and frequency instability that conclusively led to blackout [39]. This study provides significant insights of applying BESS to improve voltage and frequency stability in a realistic power system. It is shown that outage events limit the maximum power transfer to 450MW in the case studies in this paper. When the amount of power exported is increased by 44%, the system becomes unstable (Figs. 13, 17(a) and 20(a)) following single or multiple transient events, and similar phenomena happened in South-Australia. From the aforementioned three case studies and simulation results with STATCOM and BESS, it is evident that BESS can potentially contribute in simultaneous voltage and frequency regulation to improve system stability and enhance power export within areas regardless of single (Fig. 15) or multiple disturbance events (Figs. 18 and 21). However, a STATCOM remains unsuccessful in achieving such an outcome (Figs. 14, 17(b) and 20(b)). Therefore, this study demonstrates that BESS can maintain system stability within the grid defined operating ranges (according to NEM) and hence such blackout incident may be avoided with the incorporation of BESS considering large-amount of power flows between inter-connected systems.

D. The Effectiveness of BESS under Other Transient Conditions

The efficacy of BESS in different transient conditions play significant role to validate the argument of BESS competence in power system application for stability enhancement. Therefore, in addition to earlier case studies, three additional case studies have been carried out to scrutinize BESS authority to mitigate instability distress while the system is exporting 650MW power and they are as follows:

1) Case IV: Temporary single-phase short circuit fault: A single-phase-ground fault is the most common disturbance in a power system. Hence, a single-phase-ground (phase-a fault) is applied at $t = 1s$ on South-West bus for $150ms$. The generator frequency response with a BESS shown in Fig. 23 indicates that BESS effectively stabilizes the post fault system responses compared to system without the BESS. In addition, BESS with lead-lag controller provide better response in contrast to a BESS with PI and PI-lead by reducing frequency oscillation at a faster rate. Since the fault is cleared after a certain period of time, the active power of BESS reduces to nearly zero once the system has been stabilized.

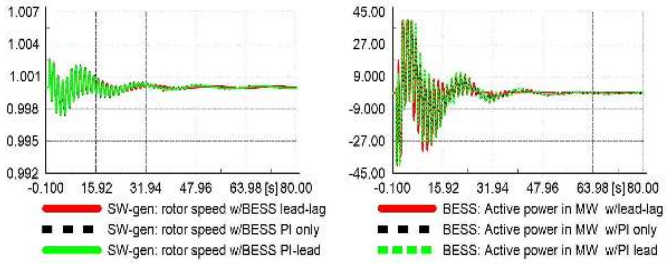

Fig. 23. The frequency of generator [p.u.] and BESS output power with temporary single-phase-ground fault

2) Case V: Permanent single-phase short circuit fault: To further investigate BESS performance in case of permanent bus fault, a permanent single-phase-ground (phase-a fault) is applied at $t = 1s$ on South-West bus. The generator frequency becomes unstable with the critical permanent single-phase-ground fault without BESS, as illustrated in Fig. 24. Hence, a BESS is installed to provide oscillation damping and to stabilize the system responses. The results illustrated in Fig. 24 indicate that BESS not only reduces oscillations right after the fault but also stabilizes the system.

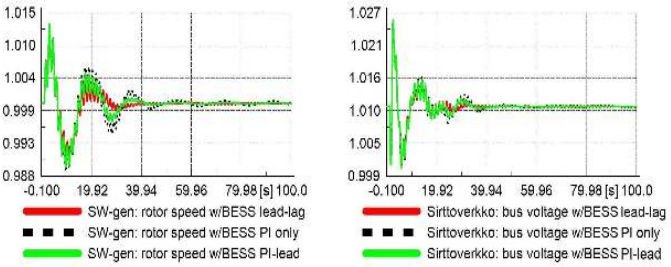

Fig. 24. The frequency of generator [p.u.] and PCC voltage [p.u.] with permanent single-phase-ground fault

In particular, BESS justifies the efficacy of enhancing transient stability performance in terms of stabilization and oscillations damping in the case of critical permanent fault. Moreover, BESS with PI-lead provides improved performance than conventional PI controlled BESS. However, BESS with lead-lag outperforms BESS with PI and PI-lead. Nevertheless, the required BESS converter size is 140MVA in comparison to 40MVA in the previous case studies. The active and reactive power of BESS reduces to zero once the system is stabilized.

3) Case VI: Without series compensation between the two systems: Series compensation significantly improves voltage stability of the system. According to the main design of the network, two connecting lines between the two systems are compensated by series compensation. To evaluate BESS competence without series compensation between these two lines, a permanent line outage at $t = 3.1s$ on N-Sirtoverkko line is applied. The system responses shown in Fig. 25 illustrate that even if there are no series compensations installed between the two interconnected systems, BESS effectively diminishes accelerating oscillations and stabilizes

the system voltage and frequency according to NEM stability requirements.

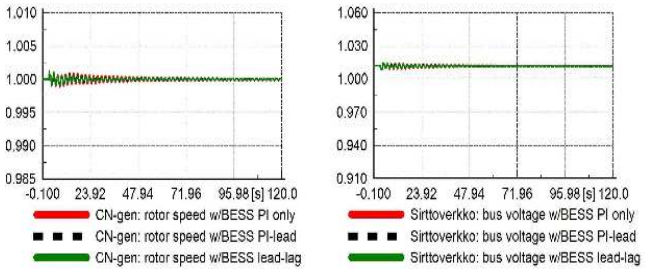

Fig. 25. The frequency of generator and PCC voltage [p.u.] w/out series compensation

E. Performance index analysis

Performance index analysis is a way of determining controller performance and robustness in achieving the desired system outcome. The sum of squared errors (SSE) is applied as performance indices to evaluate the proposed controllers effectiveness in tracking set point.

$$SSE = \sum_{k=1}^{n} (x_k - y_k)^2 \tag{10}$$

where, x_k=initial steady state value and y_k= real empirical k^{th} value.

The SSE calculation of voltage and frequency for Cases I, II & V in Table I shows that, the proposed PI-lead and lead-lag controlled BESS has smaller SSE value that demonstrates better performance of the proposed controllers than conventional PI controlled BESS. Similar performance of the proposed controller is also observed in other case studies. Moreover, lead-lag controlled BESS exhibits improved performance than BESS with all other controllers.

TABLE I
INDIVIDUAL CONTROLLER PERFORMANCE ANALYSIS ACCORDING TO SSE

	PI-only	PI-lead	Lead-lag	Observation
Case I	0.001171	0.000819	0.000621	frequency
	0.002051	0.001602	0.001244	voltage
Case II	0.001127	0.000804	0.000633	frequency
	0.001904	0.001501	0.001207	voltage
Case V	0.062582	0.053704	0.050276	frequency
	0.05222	0.048938	0.048168	voltage

From the multiple simulation studies and post fault transient dynamics with STATCOM and BESS, it is evident that BESS, installed at the same location for all case studies, is effective in maintaining transient stability by providing required oscillation damping following various levels of temporary and permanent faults. Moreover, the proposed BESS with PI-lead and lead-lag control strategies provides improved transient performance in mitigating instability problem as compared to traditional PI controlled BESS.

V. CONCLUSION

In this research, BESS with PI-lead and lead-lag controller design methods are proposed to support transient voltage and frequency regulation and strengthen power exports between the two large-scale interconnected power systems. The effectiveness of the proposed controllers are compared and demonstrated with the conventional PI controlled BESS and state-of-the-art STATCOM technology. Detailed modeling of BESS with the proposed controllers and the dynamic performance of STATCOM and BESS in regulating and enhancing transient responses are demonstrated and discussed. The following can be summarized from the presented studies:

- During a permanent network fault, there is a limit of maximum power export between two interconnected power systems and beyond that limit, the system lost its stability without additional damping support.
- When considering instability phenomena, it is observed that STATCOM failed to provide supplementary system damping whereas BESS with simultaneous voltage and frequency regulating ability ensures transient stability and dynamic security of the power system. The dynamic simulation results evidently indicate that BESS is capable of providing sufficient power system damping, enhancing the transient stability of two interconnected large-scale power systems in a multi-machine environment and enhancing 44.44% higher amount of power export in contrast to normal power transfer limit. It is also observed that the changes in battery SOC are minimum as high power is more imperative than energy capacity.
- This study provides the convincing recognition of BESS competence in avoiding voltage and frequency collapse and thus could prevent the potential blackout in real power system such as the outage happened in South-Australia.
- Moreover, BESS with lead-lag controller demonstrates better performance compare to both conventional PI and PI-lead controller in terms of faster settling time and smaller oscillation and provide smoother response once the system stability is achieved in all case studies. In addition, SSE based performance index analysis also rationalizes improved performance of lead-lag controlled BESS.
- Considering the non-stationary behaviors of power system, BESS has been proven to be effective in enhancing transient stability in multiple temporary and permanent disturbance occasions and allowing to make use of available transmission capacity.

Hence, it can be concluded that the proposed PI-lead and lead-lag control strategies for BESS not only contributes in oscillation damping to stabilize the unstable system in contrast to STATCOM but also outperforms conventional PI controlled BESS. Finally, it is recognized that increased penetration level of low inertial RES may have additional impacts on power system oscillation damping during transient events which can significantly affect power system stability. Future study will focus on the impact of low inertia due to RES penetration on power system dynamic performance and power transfer

capability across interconnected network and BESS efficacy in such circumstances. Also, coordinated control of synchronous machine and BESS in other network events will be carried out to analyze BESS effectiveness. Moreover, intelligent control strategies and controller robustness is bounded to get further attention in future development of BESS control strategies.

APPENDIX A
SYSTEM PARAMETER

Capacitor parameters: Cap-Siirto-N= Cap-CN-NW=106 μF, Cap-NW-Siirto=114.83 μF, Cap-C-CN= Cap-C-CN-1=62.63 μF, Cap-CN-N=81.06 μF

BATTERY PARAMETER

Capacity/Cell-30 Ah, Empty cell minimum voltage-22 V, Full cell voltage-13.85 V, Cells in parallel-60, Cells in row-65, Nominal source voltage-0.9 kV, Resistance/cell-0.001 ohm.

CONTROLLERS PARAMETER

PI controller: T_p=0.01, T_q=0.02, K_d=K_q=1, T_{id}=4, T_{iq}=4, i_{d-max}=i_{q-max}=1, i_{d-min}=i_{q-min}=-1.

PI-lead controller: T_p=0.01, T_q=0.02, T_{b1}=T_{b2}=1, T_{a1}=T_{a2}=0.5, K_d=K_q=1, T_{id}=4, T_{iq}=4, i_{d-max}=1, i_{d-min}=i_{q-min}=-1.

Lead-lag controller: T=6; T_{z1}=1, T_{p1}=0.5, T_{z2}=4, T_{p2}=15, T_{z3}=1, T_{p3}=0.5, T_{z4}=4, T_{p4}=15, K_P=K_Q=5, i_{d-max}=i_{q-max}=1, i_{d-min}=i_{q-min}=-1.

TABLE II
LOAD PARAMETER

Load	MW	MVar	Load	MW	MVar
South-West	570	250	Central-South	485	150
South	570	250	Central-North	570	250
South-East	570	250	North	135	50
Central	428	0	North-East	135	50
Central-East	285	100	North-West	285	50
Central-West	428	150			

TABLE III
GENERATOR ACTIVE AND REACTIVE POWER PARAMETERS:

South-West	481	-137	Central-East	285	-210
South	570	-87	Central-North	570	-170
South-East	570	30	North	85	-144
Wind-S	200	0	North-East	85	-75
Wind-SE	100	0	Wind-NE	50	0
Central	428	-336	North-West	285	-184
Wind-C	100	0	Nordic N2	0	-163
Central-West	428	-144	Nordic N1	0	0
Wind-CW	50	0	Nordic C	0	0
Central-South	285	-251	Nordic S	0	-585

REFERENCES

[1] B. S. Joshi, O. P. Mahela, and S. R. Ola, "Reactive power flow control using static var compensator to improve voltage stability in transmission system," in *2016 International Conference on Recent Advances and Innovations in Engineering (ICRAIE)*, Dec 2016, pp. 1–5.

[2] C. R. Fuerte-Esquivel and E. Acha, "Newton-raphson algorithm for the reliable solution of large power networks with embedded FACTS devices," *IEE Proceedings - Generation, Transmission and Distribution*, vol. 143, no. 5, pp. 447–454, Sep 1996.

[3] M. Yesilbudak, S. Ermis, and R. Bayindir, "Investigation of the effects of FACTS devices on the voltage stability of power systems," in *2017 IEEE 6th International Conference on Renewable Energy Research and Applications (ICRERA)*, Nov 2017, pp. 1080–1085.

[4] A. Abu-Siada and C. Karunar, "Transmission line power transfer capability improvement, case study," *IFAC Proceedings Volumes*, vol. 45, no. 21, pp. 495 – 499, 2012, 8th Power Plant and Power System Control Symposium.

[5] M. Kolcun, Z. Conka, L. Beňna, M. Kanáalik, and D. Medveďd, "Improvement of transmission capacity by FACTS devices in central east europe power system," *IFAC-PapersOnLine*, vol. 49, no. 27, pp. 376 – 381, 2016, iFAC Workshop on Control of Transmission and Distribution Smart Grids CTDSG 2016.

[6] K. Karthikeyan and P. Dhal, "Transient stability enhancement by optimal location and tuning of STATCOM using pso," *Procedia Technology*, vol. 21, pp. 345 – 351, 2015.

[7] M. Darabian and A. Jalilvand, "Improving power system stability in the presence of wind farms using STATCOM and predictive control strategy," *IET Renewable Power Generation*, vol. 12, no. 1, pp. 98–111, 2018.

[8] L. M. Castro, E. Acha, and C. R. Fuerte-Esquivel, "A novel STATCOM model for dynamic power system simulations," *IEEE Transactions on Power Systems*, vol. 28, no. 3, pp. 3145–3154, Aug 2013.

[9] G. Cakir and G. Radman, "Placement and performance analysis of STATCOM and SVC for damping oscillation," in *2013 3rd International Conference on Electric Power and Energy Conversion Systems*, Oct 2013, pp. 1–5.

[10] S. Bagchi, R. Bhaduri, P. N. Das, and S. Banerjee, "Analysis of power transfer capability of a long transmission line using FACTS devices," in *2015 International Conference on Advances in Computing, Communications and Informatics (ICACCI)*, Aug 2015, pp. 601–606.

[11] J. Servotte, E. Acha, and L. M. Castro, "Smart frequency control in power transmission systems using a BESS," in *2015 IEEE Innovative Smart Grid Technologies - Asia (ISGT ASIA)*, Nov 2015, pp. 1–7.

[12] A. V. Savkin, M. Khalid, and V. G. Agelidis, "A constrained monotonic charging/discharging strategy for optimal capacity of battery energy storage supporting wind farms," *IEEE Transactions on Sustainable Energy*, vol. 7, no. 3, pp. 1224–1231, July 2016.

[13] K. Kawabe and A. Yokoyama, "Effective utilization of large-capacity battery systems for transient stability improvement in multi-machine power system," in *2011 IEEE Trondheim PowerTech*, June 2011, pp. 1–6.

[14] H. Setiadi, N. Mithulananthan, and M. J. Hossain, "Impact of battery energy storage systems on electromechanical oscillations in power systems," in *2017 IEEE Power Energy Society General Meeting*, July 2017, pp. 1–5.

[15] H. Maleki and R. K. Varma, "Comparative study for improving damping oscillation of SMIB system with STATCOM and BESS using remote and local signal," in *2015 IEEE 28th Canadian Conference on Electrical and Computer Engineering (CCECE)*, May 2015, pp. 265–270.

[16] M. J. Hossain, H. R. Pota, and R. A. Ramos, "Improved low-voltage-ride-through capability of fixedspeed wind turbines using decentralised control of STATCOM with energy storage system," *IET Generation, Transmission Distribution*, vol. 6, no. 8, pp. 719–730, August 2012.

[17] A. Chakraborty, S. K. Musunuri, A. K. Srivastava, and A. K. Kondabathini, "Integrating STATCOM and battery energy storage system for power system transient stability: A review and application," *Advances in Power Electronics*, vol. 2012, 2012.

[18] J. Aguado, S. de la Torre, and A. Triviño, "Battery energy storage systems in transmission network expansion planning," *Electric Power Systems Research*, vol. 145, pp. 63 – 72, 2017.

[19] U. Datta, A. Kalam, and J. Shi, "Battery energy storage system for transient frequency stability enhancement of a large-scale power system," in *2017 Australasian Universities Power Engineering Conference (AUPEC)*, Nov 2017, pp. 1–5.

[20] A. Kanchanaharuthai, V. Chankong, and K. A. Loparo, "Transient stability and voltage regulation in multimachine power systems vis-a'-vis STATCOM and battery energy storage," *IEEE Transactions on Power Systems*, vol. 30, no. 5, pp. 2404–2416, Sept 2015.

[21] M. Beza and M. Bongiorno, "An adaptive power oscillation damping controller by STATCOM with energy storage," *IEEE Transactions on Power Systems*, vol. 30, no. 1, pp. 484–493, Jan 2015.

[22] B. Jena and A. Choudhury, "Voltage and frequency stabilisation in a micro-hydro-PV based hybrid microgrid using FLC based STATCOM equipped with BESS," in *2017 International Conference on Circuit ,Power and Computing Technologies (ICCPCT)*, April 2017, pp. 1–7.

[23] J. Park, J. Yu, J. Kim, M. Kim, K. Kim, and S. Han, "Frequency/Voltage regulation with STATCOM with battery in high voltage transmission system," *IFAC-PapersOnLine*, vol. 49, no. 27, pp. 296 – 300, 2016, iFAC Workshop on Control of Transmission and Distribution Smart Grids CTDSG 2016.

[24] B. Singh and Z. Hussain, "Application of Battery Energy Storage System (BESS) in voltage control and damping of power oscillations," in *2010 5th International Conference on Industrial and Information Systems*, July 2010, pp. 514–519.

[25] X. Xu, M. Bishop, D. G. Oikarinen, and C. Hao, "Application and modeling of battery energy storage in power systems," *CSEE Journal of Power and Energy Systems*, vol. 2, no. 3, pp. 82–90, Sept 2016.

[26] Y. Ge, W. Du, and T. Littler, "Applying STATCOM/BESS stabilizers in a real large-scale power system," in *2nd IET Renewable Power Generation Conference (RPG 2013)*, Sept 2013, pp. 1–4.

[27] NEM, "The Frequency Operating Standard-stage one final, [Available Online]:https://www.aemc.gov.au/sites/default/files/content/c2716a96-e099-441d-9e46-8ac05d36f5a7/rel0065-the-frequency-operating-standard-stage-one-final-for-publi.pdf, [Accessed on: 2018-06-08]."

[28] NEM/AEMO, "Generator technical requirements, [Available Online]:https://www.aemo.com.au/-/media/files/electricity/nem/security_and_reliability/reports/2017/aemo-gtr-rcp-110817.pdf, [Accessed on: 2018-06-08]."

[29] Anti-Windup, "Integral Anti-Windup for PI Controllers, [Available Online]:https://www.scribd.com/document/181677842/anti-windup, [Accessed on: 2018-06-09]."

[30] A. Visioli, "Modified anti-windup scheme for PID controllers," *IEE Proceedings - Control Theory and Applications*, vol. 150, no. 1, pp. 49–54, Jan 2003.

[31] ControlTheoryPro, "PI-Lead Control, [Available Online]:http://wikis.controltheorypro.com/pi-lead_control, [Accessed on: 2018-06-09]."

[32] Z. K. Jadoon, S. Shakeel, A. Saleem, A. Khaqan, S. Shuja, Q. Hasan, S. A. Malik, and R. A. Riaz., "A comparative analysis of PID, lead, lag, lead-lag, and cascaded lead controllers for a drug infusion system," *Journal of Healthcare Engineering*, vol. 2017, Jan 2017.

[33] G. Xu, L. Xu, and J. Morrow, "Power oscillation damping using wind turbines with energy storage systems," *IET Renewable Power Generation*, vol. 7, no. 5, pp. 449–457, Sept 2013.

[34] M. Chen and G. A. Rincon-Mora, "Accurate electrical battery model capable of predicting runtime and I-V performance," *IEEE Transactions on Energy Conversion*, vol. 21, no. 2, pp. 504–511, June 2006.

[35] U. Datta, "Enhanced operational performance of siirtoverkkomalli using static compensators and bess equipment," Master's thesis, Tampere University of Technology, Aug, 2016.

[36] D. GmBH, "Power Equipment Models, [Available Online]:https://www.digsilent.de/en/faq-reader-powerfactory/do-you-have-a-model-for-a-statcom-2/searchfaq/statcom.html, [Accessed on: 2018-06-01]."

[37] AEMO, "Victorian transfer limit advice – outages, [Available Online]:https://www.aemo.com.au/-/media/files/electricity/nem/security_and_reliability/congestion-information/2017/victorian-transfer-limit-advice---outages-v5.pdf, [Accessed on: 2018-06-08]."

[38] AEMO/NEM, "Transfer limit advice – NEM oscillatory stability, [Available Online]:https://www.aemo.com.au/-/media/files/electricity/nem/security_and_reliability/congestion-information/2017/transfer-limit-advice---nem-oscillatory-stability-v3.pdf, [Accessed on: 2018-06-08]."

[39] AEMO/SA, "Black system South Australia 28 September 2016, [Available Online]:https://www.aemo.com.au/-/media/files/electricity/nem/market_notices_and_events/power_system_incident_reports/2017/integrated-final-report-sa-black-system-28-september-2016.pdf, [Accessed on: 2018-06-08]."

Ujjwal Datta received the Bachelor of Science (Honours) in Electrical and Electronic Engineering from Stamford University, Bangladesh and Master of Science in Smart Grid with distinction from Tampere University of Technology, Finland. Currently he is continuing studies towards PhD at Victoria University, Melbourne, Australia. His research interests are power system stability, FACTS devices, Battery energy storage system, smart grid, home energy management system, EV and renewable energy system.

Akhtar Kalam is a Professor at Victoria University (VU), Melbourne since 1985 and a former Deputy Dean of the Faculty of Health, Engineering and Science. He is currently the Head of Engineering and Director of Externalization at the College of Engineering and Science, VU. He is also the current Chair of the Academic Board and lectures in the Masters by coursework program in the Engineering Institute of Technology, Perth, Australia. Again he is the Editor in Chief of Australian Journal of Electrical & Electronics Engineering. Further he has Distinguished Professorship position at the University of New South Wales, Sydney, Australia; MRS Punjab Technical University – Bhatinda, India; Crescent University – Chennai, India; VIT – Vellore, India and 5 Malaysian universities. He has wide experience in educational institutions and industry across four continents. He received his B.Sc. and B.Sc. Engineering from Calcutta University and Aligarh Muslim University, India. He completed his MS and Ph.D. at the University of Oklahoma, USA and the University of Bath, UK. His major areas of interests are power system analysis, communication, control, protection, renewable energy, smart grid, IEC61850 implementation and co-generation systems. He provides consultancy for major electrical utilities, manufacturers and other industry bodies in his field of expertise. Professor Kalam is a Fellow of EA, IET, AIE, a life member of IEEE and a member CIGRE AP B5 Study Committee.

Dr. Juan Shi received the Bachelor of Engineering (Honours) in Electrical Engineering from Northeastern University, China, in 1988 and the PhD degree in Electrical Engineering from Victoria University (VU), Melbourne, Australia, in 1995. Dr Shi received the Graduate Certificate in Tertiary Education from VU in 2003. She joined VU as a Lecturer in 1994, where she is currently an Associate Professor in the College of Engineering & Science. Her current research interests include automatic control and applications, power system stability, intelligent control and applications to smart energy systems, system identification, and engineering education.